Beam dynamics issues in the NSCL coupled cyclotron upgrade

F. Marti, H.G. Blosser, M.M. Gordon,T.L. Grimm, D.O. Jeon†, D.A. Johnson,
P.S. Miller, D. Poe, S. Snyder††, X.Y. Wu and R. C. York

NSCL, Michigan State University, East Lansing, MI 48824, USA

The NSCL has embarked on the upgrade of its facilities to increase the intensity of the primary beams, mainly to increase the rates of the radioactive secondary beams produced by the projectile fragmentation method. The extracted beam power is expected to reach 4 kW. This level of power in heavy ion beams is difficult to handle because of the short range of the ions. Compact superconducting cyclotrons have inherent size constraints that make it more difficult to deal with beam losses and power dissipation. Short beam bunches are desirable to minimize losses at extraction, however, with intense beams the space charge forces will limit the minimum turn width. We present the results of simulations of the different areas of the upgrade: injection, acceleration and extraction in the K500 and K1200 cyclotrons, that allow us to estimate the losses expected in the entire system.

1 Introduction

1.1 Overview

In December of 1996 the US National Science Foundation approved the proposed upgrade of the National Superconducting Cyclotron Laboratory at Michigan State University (see [1],[2]). This project had been given high priority by the Nuclear Science Long Range Planning Report [3] based on the opportunities it will create for the study of exotic beams. After the upgrade the Laboratory will operate a set of ECR ion sources, injecting into the modified K500 cyclotron. The beam extracted from the K500 will be injected by stripping into the K1200 cyclotron. After extraction from the K1200 a new fragment separator (A1900) will select the desired radioactive species produced in a thin target and transport them to the experimental vaults.

1.2 Upgrade goals

With radioactive beam production being the major aim of the project, our main goal is to reach 6.10^{12} pps for the ligth ions with energies of up to 200 MeV/u. On the other hand for heavier elements (Au-U) we expect energies close to 90 MeV/u. Our separate transmission estimates when multiplied together yield a 2 % efficiency (source to K1200 extracted beam). This number must be multiplied by the stripping efficiency that depends on each ion and charge state.

2 Challenges

2.1 Extraction system

The performance of the extraction septum in the K1200 cyclotron is the most challenging technical problem associated with the NSCL upgrade. The beam dynamics issues discussed below have been driven by the need to decrease the losses on the extraction system. The extraction systems of our two cylotrons are very similar. We will describe the K1200 system since it is the most complicated and critical for our project. Figure 1 shows the median plane cross section of the K1200 with its 3 hills and 3 valleys. The radius at extraction is 1 m. The outside yoke radius is 2.2 m. The extraction process is started by inducing a coherent precession of the beam when it crosses the $\nu_r = 1$ resonance just before extraction. The precession is produced by a first harmonic field imperfection created by a set of trim coils. The amplitude and phase of the field imperfection are set to

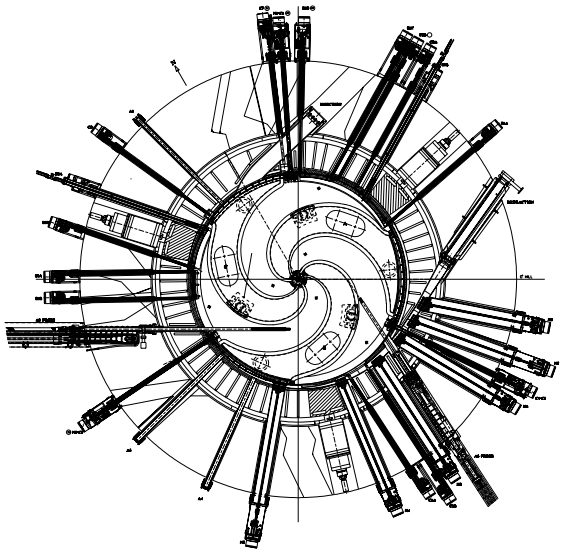

Figure 1: Mid-plane section of the K1200 showing the multiple drives associated with the extraction system elements.

induce a separation between central rays of consecutive turns of approximately 3-4 mm (the normal radius gain per turn is less than 1 mm near extraction). Larger precession amplitudes induce excessive beam phase space deformations due to non-linearities. As the beam size is approximately 3 mm, a small turn separation exists for particles at the center of the rf phase distribution. The first component of the extraction system is an electrostatic deflector (see vertical cross section in figure 2) approximately 1 m long. This deflector operates at electric fields of up to 130 kV/cm on a horizontal gap of 6 mm. The deflector is split longitudinally in three sections that are hinged at the high voltage electrode. By changing the relative position of the three sections the deflector shape is adapted to different beams. The major losses in the extraction process occur at the entrance of this first deflector. A second electrostatic deflector follows and then the beam goes through a set of focusing bars that compensate for the strong radial defocusing of the cyclotron fringe field.

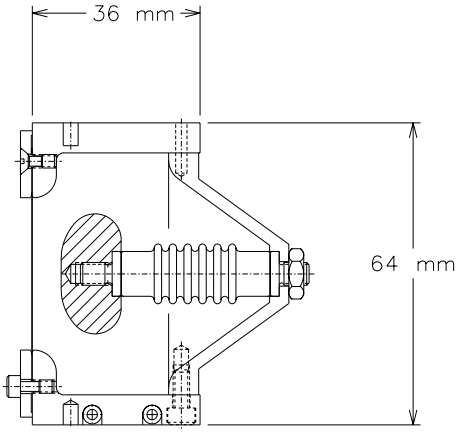

Figure 2: Vertical cross section of the K1200 deflector, showing the thin (0.25 mm) septum on the left. The gap between the septum and the high voltage electrode is 6 mm.

The major difficulty associated with the extraction of high intensity heavy ions (compared with the extraction of protons for example) comes from the very short range of the heavy ions in the materials used for deflector septa. We show in figure 3 the energy loss of an 8 GeV total energy argon ion in tungsten. The range is just over 3 mm. Our proposed beams will reach extracted beam powers of 4 kW, with 10 % losses, approximately 400 W will be absorbed on a volume of 4 mm (beam height) x 3 mm (beam range) x 0.25 mm (septum thickness). The best candidates for septum materials are pyrolytic graphite and tungsten. The pyrolytic graphite has a superior heat conductivity in the direction of the layers, low residual radioactivity and longer range than tungsten. Tungsten, on the other hand, does not decrease the voltage holding capabilities of the deflector as graphite does (we are still investigating techniques to mitigate this negative effect, see [4]). Thermomechanical calculations have shown that notched tungsten sheets can be used at 400 W power level [5] and septa have been operated at levels up to 500 W.

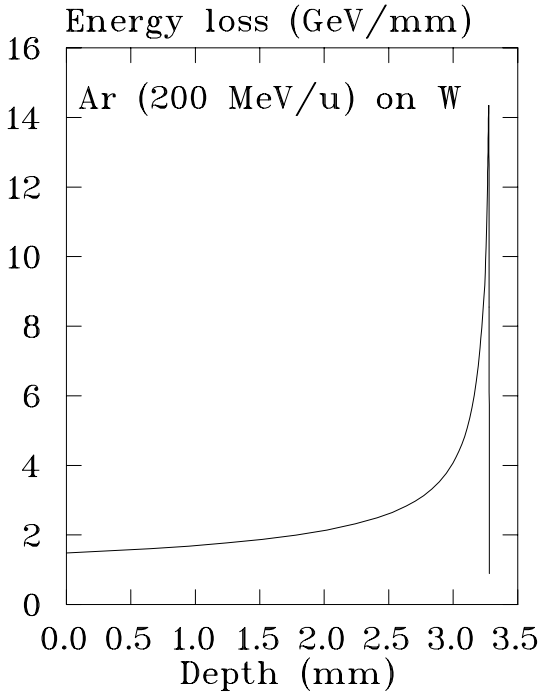

Figure 3: Energy loss for an 8 GeV total energy argon beam on a tungsten septum.

2.2 K500 magnetic field

As part of the implementation of the NSCL upgrade the K500 cyclotron has been rotated 120 degrees (natural symmetry of the 3-sector magnet) to direct the extracted beam toward the K1200 cyclotron. As the cyclotron had to be dissasembled in this process we could use this opportunity to correct some of the problems associated with magnetic field imperfections. The original configuration did not allow us to run at high excitations (4-5 T) with the coil centered on the steel center; decentering forces from yoke and cryostat imperfections were too large, forcing us to position the superconducting coils 1 mm off-center. This created a strong (over 20 gauss) first harmonic that depended on the operating point and that had to be partially compensated with the field bump produced by trim coil 13, which was also used to induce a precession at ν_r=1 before extraction. The details of

this compensation have been studied in [6] and [7].

During our reassembly we compensated the steel assymetries in the K500 yoke where this first harmonic originated. It was a laborious fine tuning process due to the small amount of steel that was needed to improve the symmetry and position the coil on center (see [8]). The resulting first harmonic over the operating region can be seen in figure 4. The amplitude is small and fairly constant at the ν_r=1 resonance radius.

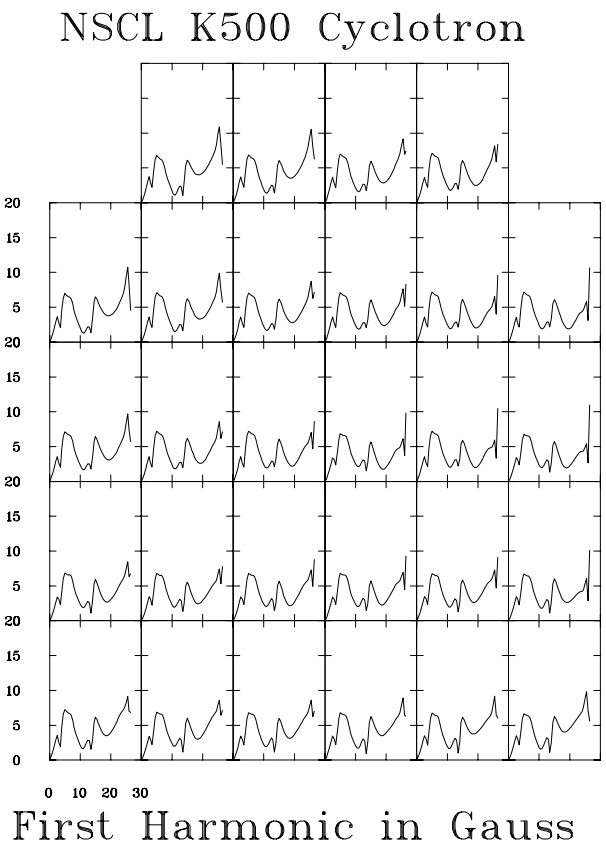

Figure 4: First harmonic imperfections in gauss vs. radius over the complete mapped grid. Maps in a horizontal row have different main coil ratios at approximately the same central field. The field increases vertically from approximately 3.0 T to 5.0 T in 0.5 T steps. We see that no large variations are present.

3 Short phase bunch operation

3.1 K500 bunch selection

The maximum beam phase width that allows separated turns in the K1200 at extraction (neglecting longitudinal space charge effects) gives a FWHM of 3 degrees. The central region of the K500 cyclotron is designed with the possibility of making a first turn coarse phase selection that would limit the phase width of the accelerating beam and complement the phase slits that operate at a radius of 7 inches. Beam simulations were performed [9] that included ray tracking from a point 3 m below the cyclotron median plane, through the main magnet solenoidal fringe field, buncher, spiral inflector, central region and up to the phase slits (but not including the effects of space charge). For an injected phase space of 75 π mm mrad the efficiency of the selection mechanism is 5.5 % (fraction of the DC beam in the 3 degree bunch), and the timing spectra are shown in figure 5. The top plot corresponds to the point in the central region just before the first turn slit, the middle plot to a point just before the phase slits, and the bottom plot after both devices.

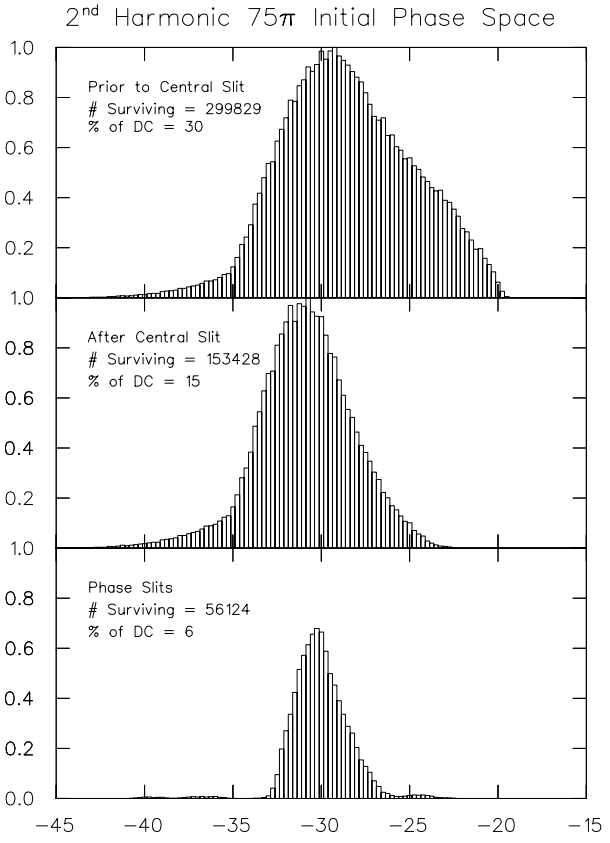

Figure 5: Timing spectra for a 75π mm mrad injected beam before the first turn slit (top), before the phase selection pins (middle) and after them (bottom) in the K500 cyclotron. The abcissa is indicated in RF degrees.

3.2 Space charge calculations

Space charge forces affect the beam behavior in two different ways. Transverse forces will increase the beam size and reduce the vertical focusing frequency. If this reduction is significant, axial beam loss could occur. Longitudinal space charge forces on the other hand increase

the energy gain of the leading edge of the bunch and reduce the energy gain of the tail of the bunch. Because of the radius-energy correlation in cyclotrons, this energy spread expands the radial region occupied by each turn, and if it becomes large enough, consecutive turns will overlap that otherwise would be separated.

3.2.1 Transverse space charge effects Two approaches have been used to estimate the transverse effect of space charge forces. Blosser and Gordon [10] used a model consisting of a uniformly charged wedge, obtaining for the limiting current that would decrease the vertical focusing frequency to zero:

$$I_{\rm lim} = (\Delta z)\nu_z^2 \omega \epsilon_o (\frac{\Delta\phi}{2\pi})(\frac{\Delta E}{Qe})$$

where Δz is the beam height, ν_z is the vertical focusing frequency, ω is the orbital angular frequency, ϵ_o is the permittivity of vacuum, $\Delta\phi$ is the full beam phase width, ΔE the energy gain per turn and Qe is the ion charge.

Joho [11] developed a model appropriate for the case of separated turns, with the following current limit:

$$I_{\rm lim} = \frac{1}{4}(\frac{A}{Q}) I_o \beta \nu_z^2 (\frac{b_{max}}{R_\infty})^2 (\frac{\Delta\phi}{2\pi})$$

where I_o= 31 MA, b_{max} is the beam half height, $R_\infty = c/\omega_o = hc/\omega_{rf}$ We have used these two models to estimate the intensity limits for both cyclotrons, K500 and K1200. The results are shown in table 1. These values indicate critical currents in any case much higher than the desired currents of 10 μA. We do not expect the transverse forces to be any problem.

	K500	K1200
Overlapping turns	86	215
Separated turns	224	7920

Table 1: Limiting currents (in μA) that would reduce the vertical focusing frequency to zero.

3.2.2 Longitudinal space charge forces Work has been performed on the calculation of longitudinal space charge forces using various models. Elaborate calculations have been presented by Adam [12]. Most of this work provides only a qualitative understanding of the space charge problems. We have used the model developed by Gordon [13],[14] to estimate the optimum phase width as a function of average current. In this model the charge distribution is divided into radial segments of width Δr equal to the radius gain per turn. During each turn the ions in one segment move outward to the next segment, and so on until they are extracted at r=r$_{max}$. At each r value the actual charge distribution is replaced by a two dimensional rectangular one having a width $\Delta y = r\Delta\theta$ and a full height Δz=2z$_0$. With $y_0 = \frac{1}{2}\Delta y$ the charge distribution along the azimuthal coordinate is assumed to be proportional to:

$$\sigma_2(y) = \frac{1}{y_0}(1 - \frac{|y|}{y_0}),$$

as shown in figure 6. In the vertical direction the charge

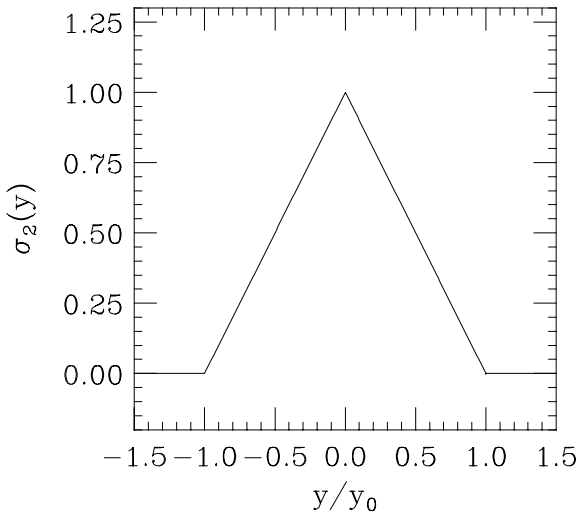

Figure 6: Charge distribution in the azimuthal direction used in the longitudinal space charge force calculations.

distribution is given by:

$$\sigma_3(z) = \frac{2}{\pi z_0}(1 - \frac{z^2}{{z_0}^2})^{1/2},$$

as results from a uniformly populated phase space ellipse, and shown in figure 7. We can then determine the electric potential of this charge distribution bounded by conducting planes at heights $z = \pm z_c$. The electric field determined from this potential distribution is used to integrate the longitudinal equations of motion from the injection point to extraction. By iterating these calculations, the program optimizes the values of the starting phase, frequency and bunch length so as to obtain the maximum beam current consistent with turn separation at the extraction energy. We present in table 2 an example for the Q/A=0.5, 200 MeV/u field. The current indicated in each column gives an energy spread for the last turn equal to 95% of the energy gain per turn. Two different dee voltages were used, 150 and 180 kV. The real K1200 magnetic field was considered (non-isochronous field) as well as an idealized perfectly isochronous field, that does not have the edge phase slip associated with real fields. We normally extract beyond the ν_r=1 resonance, at approximately ν_r=0.8.

	Isochronous Field		Non-isochronous Field	
V_d (kV)	150	180	150	180
qV_0 (keV/u)	225	270	225	270
$I_{critical}$ ($e\mu$A)	4.3	8.3	3.6	7.5
$\Delta\phi$	4.2°	4.4°	4.2°	4.4°
ϕ_{ci}	0°	0°	−15°	−11°
ϕ_{cf}	−1.66°	−2.04°	8.97°	4.09°
Turn Number	817.9	681.6	899.8	724.4
ΔRF (kHz)	−0.149	−0.221	2.81	2.29

Table 2: Optimized solutions of short bunch acceleration for the K1200 Q/A=0.5, 200 MeV/u beam. The critical current produces an energy spread in the last turn equal to 95% of the energy gain per turn. ϕ_{ci} and ϕ_{cf} are the central ray initial and final phases. The beam height is $2z_0$=5 mm and z_c=13 mm.

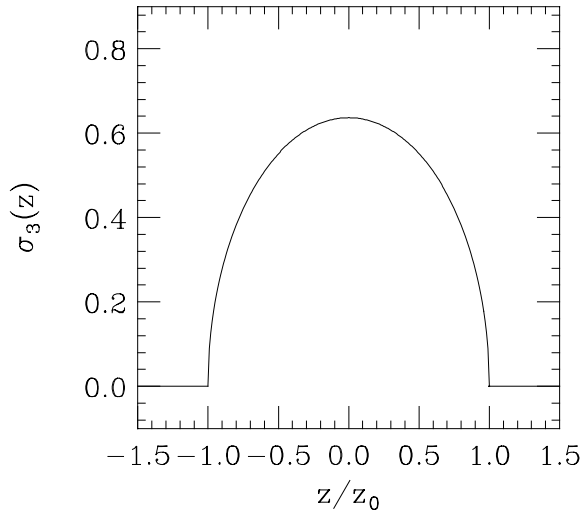

Figure 7: Charge distribution in the vertical direction used in the longitudinal space charge force calculations.

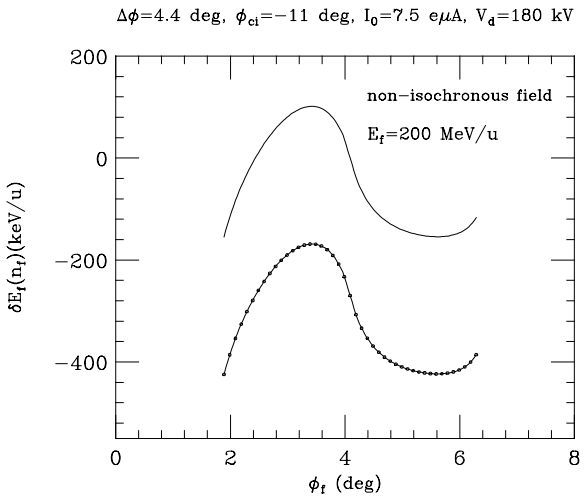

Figure 8: Energy spread bands for the last and the next-to-last turns in the K1200 cyclotron at the critical intensity under longitudinal space charge forces.

The energy distribution of the last two turns for the non-isochronous case on the 4th column of table 2 is shown in figure 8. The energy of the central ray in the last turn is taken as zero. We see that for the critical current the energy spread bands almost overlap.

It is interesting to study the energy spread as a function of current for different voltages. Joho showed in [11] that the energy spread is proportional to the average current and proportional to the square of the turn number (n). This dependence on n^2 can be interpreted as one factor coming from the time that the space charge forces act and the other from the increased current density. If we now apply this to the energy gain per turn we obtain:

$$\frac{\Delta E_{SC}}{\Delta E_1} \propto In^3$$

Figure 9 shows the energy spread normalized to the energy gain per turn for the K1200 Q/A=0.5, 200 MeV/u field. We see the almost linear dependence on the current and the cubic dependence on the dee voltageV_d.

We find that the current limits obtained from our simulations of the longitudinal motion are not very far below the desired current (10μA). Given the relative simplicity of the model we have used, these results are encouraging, especially since the only available measurements [13] showed that the actual space charge effect is only about one half that predicted by our model. Nevertheless, we decided for security to investigate the simpler operating mode presently used in the K1200 which does not require short bunches, namely, multiturn extraction with relatively large phase widths.

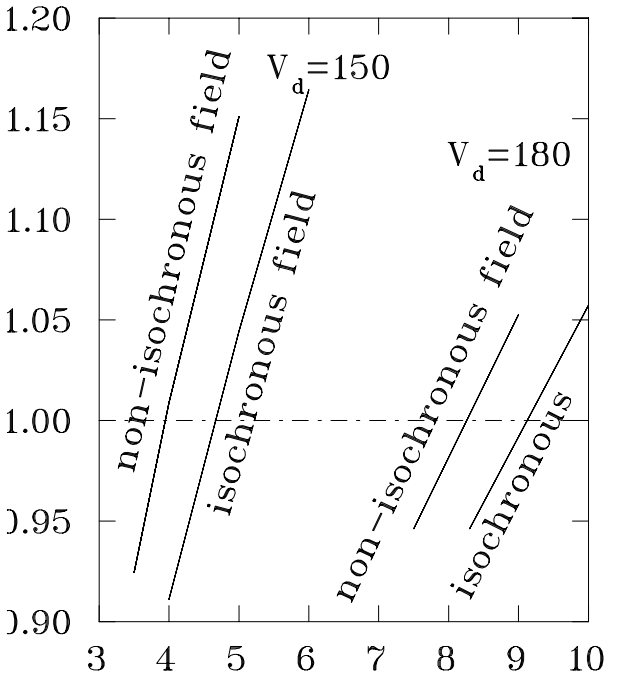

Figure 9: Energy spread in the last turn ($\Delta E_{SC}/\Delta E_1$) as a function of the beam current (μA) for the Q/A=0.5, 200 MeV/u field in the K1200. Two different dee voltages (150 and 180 kV) are considered. A non-isochronous as well as an isochronous field were considered.

4 Broad phase bunch option

4.1 K1200 extraction estimates

Extensive calculations were performed [15] of the extraction process in the K1200 cyclotron. The purpose was to understand the relatively low (about 50%) extraction efficiency presently achieved in the cyclotron for some ions and guide our improvement plan to obtain better performance. The calculations simulated the acceleration of ensembles of particles with different phase ranges from the central region out through the extraction system including field imperfections and realistic thicknesses of the extraction septum. Two different phase space emittances (3 and 12 mm mrad unnormalized at extraction) were considered in both radial and vertical planes. These calculations did not include space charge effects, because we concentrated on long bunches (20 RF degrees) where the space charge forces should be insignificant. We show in figure 10 the histogram of the number of particles per bin (Δr=0.0055 inch) for the case of the small z ellipse and a centered beam. The deflector position is at 39.87 inches. Two coherent precession loops (produced by the field bump at ν_r=1) are visible before the septum, at 39.4 and 39.75 approximately. Three different septum thicknesses were considered, 0.125, 0.25 and 0.5 mm (our present deflector uses a 0.25 mm septum). Extraction efficiencies are summarized in table 3. More detailed discussion of phase space distribution and energy spread are given in another paper [15].

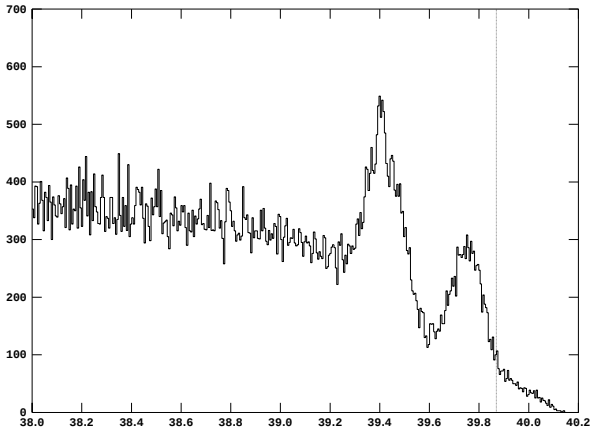

Figure 10: Histogram of the number of particles vs. radius (between 38. and 40.2 inches. There are 400 bins of 0.0055 inches width each. The ions included a 12 mm mrad ellipse in r and a 3 mm mrad ellipse in z.

	Septum thickness (mm)		
	0.125	0.25	0.5
ϵ_r=12 mm mrad ϵ_z= 3 mm mrad centered beam	88	84	78
ϵ_r=12 mm mrad ϵ_z=12 mm mrad centered beam	83	79	72
ϵ_r=12 mm mrad ϵ_z= 3 mm mrad off-centered beam	76	71	62
ϵ_r=12 mm mrad ϵ_z=12 mm mrad off-centered beam	61	57	50

Table 3: Extraction efficiencies through the first electrostatic deflector in percent resulting from the simulations for different combinations of phase space sizes and beam on and off-center.

From the results listed in table 3 we see that the larger phase space results with an off-centered beam agree quite well with our observed extraction efficiencies of 50-65 %. On the other hand our best experimental results (80 %) agree with the larger phase spaces with a centered beam. Our experimental observations of the beam centering with a TV probe confirmed that when we obtained the higher efficiency, the beam was extremely well

centered. Preliminary experiments with phase space reduction in our present axial injection system confirmed the increased extraction efficiencies for beams where the transverse phase space had been reduced from our normal operating mode.

5 Conclusions

We have evaluated two different modes of operation of the K1200 cyclotron in the booster mode for high intensity production of radioactive beams. In the short bunch mode (3 degrees RF) we found that the longitudinal space charge forces would probably prevent us from having separated turns at extraction at the dee voltage levels that we presently achieve. In the broad bunch mode we have found that extraction efficiencies of 88 % are possible with centered beams and limited transverse phase spaces. This second mode is our preferred mode because of the more relaxed tolerances and stability requirements. Increasing the brightness of the beam and limiting the halo should improve our extraction efficiency.

Acknowledgements. Work supported by NSF Grant PHY-95-28844

† Present address: IUCF, Bloomington, IN.
†† Present address: Science City at Union Station, Kansas City, MO

References

[1] F. Marti et al., Proc. of the 14th Intl. Conf. on Cyclotrons and Their Appl., Cape Town, 1995, 45.

[2] R. C. York et al., The NSCL Coupled Cyclotron Project - Overview and Status,this conference.

[3] Nuclear Science: A Long Range Plan, DOE/NSF Nuclear Science Advisory Commottee, February 1996.

[4] D. Poe et al., this conference.

[5] J. DeKamp and F. Marti, in Proc. 1997 PAC, Vancouver.

[6] F. Marti, H.G. Blosser and M.M. Gordon, Proc. of the 10th Intl. Conf. on Cyclotrons and Their Appl., East Lansing, 1984, 44.

[7] F. Marti and P. Miller, Proc. of the 10th Intl. Conf. on Cyclotrons and Their Appl., East Lansing, 1984, 107.

[8] T.L. Grimm et al., Compensation of magnetic field imperfections in the NSCL K500 superconducting cyclotron, this conference.

[9] S. Snyder. *Study and redesign of the NSCL K500 injection, central region and phase selection systems.* PhD thesis, Michigan State University, 1995.

[10] H.G. Blosser and M.M. Gordon, Nucl. Instrum. Meth. **13**, 101 (1961).

[11] W. Joho, Proc. of the 9th Intl. Conf. on Cyclotrons and Their Appl., Caen, 1981, 337.

[12] S. Adam, Proc. of the 14th Intl. Conf. on Cyclotrons and Their Appl., Cape Town, 1995, 446.

[13] M.M. Gordon in Proc. of the 5th Intl. Conf. on Cyclotrons and Their Appl., Oxford, 1969, 305.

[14] M.M. Gordon and D.O. Jeon, Research Note 12/95.

[15] H.G. Blosser, D.A. Johnson and F. Marti, Numerical Study of Efficiency of Multi-turn Extraction in the K1200 Cyclotron, this conference.